Robust Design of Compressor Fan Blades Against Erosion

Apurva Kumar

Andy J. Keane

Prasanth B. Nair[1]
e-mail: p.b.nair@soton.ac.uk

Computational Engineering and Design Group,
School of Engineering Sciences,
University of Southampton,
Highfield, Southampton SO17 1BJ, UK

Shahrokh Shahpar
Aerothermal Methods,
Rolls-Royce Plc. Derby,
DE24 8BJ, UK

This paper is concerned with robust aerodynamic design of compressor blades against erosion. The proposed approach combines a multiobjective genetic algorithm with geometry modeling methods, high-fidelity computational fluid dynamics, and surrogate models to arrive at robust designs on a limited computational budget. The multiobjective formulation used here allows explicit trade-off between the mean and variance of the performance to be carried out. Detailed numerical studies are presented for robust geometric design of a typical compressor fan blade section to illustrate the proposed methodology. The performance of a selected robust optimal solution on the Pareto front is compared to a deterministic optimal solution to demonstrate that significant improvements in the mean shift and variance can be achieved. [DOI: 10.1115/1.2202886]

Keywords: robust design, multiobjective optimization, surrogate modeling, compressor blades, erosion

1 Introduction

During operation, compressor fan blades are exposed to a number of erosion processes [1] which can lead to reduction of the blade chord, alteration in the shape, and increase in the surface roughness [2]. This is critical to the blade performance and can lead to degraded overall engine efficiency. Roberts [3] has shown that geometric variability in the form of leading edge erosion in compressor airfoils may account for an increase of 3% or more on the thrust specific fuel consumption. Erosion can cause up to 6% deterioration in total pressure loss of compressor fan blades [4]. Replacing the eroded compressor fan blades can prove to be expensive. Hence, it is desirable to design compressor fan blades that are robust to erosion processes, i.e., blades whose performance does not degrade significantly in the presence of erosion.

Traditional deterministic optimization methods seek to optimize the nominal performance of the system. These methods when applied to product design tend to produce solutions that perform well at the design point but have poor off-design characteristics. In recent years, there has been a resurgent interest in computational analysis and design methods that rationally accommodate uncertainty arising from sources such as varying operating conditions, manufacturing errors, or inaccurate system parameters [5]. In most cases, removing the causes of uncertainty can be prohibitively expensive. Robust design is concerned with minimizing the effect of uncertainty on design performance without eliminating the source of uncertainty [6].

In the 1970s Taguchi emphasized the need to reduce variation in product and processes to improve their quality [7,8]. An overview of Taguchi's experimentation strategy and parameter design method can be found in Refs. [9,10]. The system design method and the selection of signal-to-noise ratio (SNR) as a measure of robustness proposed by Taguchi had several limitations [11,12]. Welch et al. [13,14] proposed a system for quality improvement via computer experiments as an alternative to Taguchi's method. Statistical decision theory has also been used to formulate robust design as an optimization problem. The minimax strategy [15] can be used to find a design with optimal worst case performance [16]. This method is conservative as it seeks to protect the decision maker against the worst case scenario [12]. Huyse et al. [17,18] used the idea of Bayes risk minimization to achieve consistent improvement of the performance over a given range of uncertainty parameters.

Many researchers have proposed to minimize a single objective to achieve robust design. These methods can be classified into two categories where the aim is to minimize (1) the expectation of the objective function in its neighborhood [19–21,18] and (2) the variance of the objective function [22,23]. Tsutsui et al. [19] used a genetic algorithm based method with perturbations in the phenotype while evaluating the function value. They call this method Genetic Algorithms with Robust Solution Searching Schemes (GAs/RS^3), which they further combine with a sharing scheme to seek multiple robust solutions. Jin et al. [24] provide a survey of evolutionary optimization based methods for seeking robust optimal designs. Garzon et al. [25] present two formulations for robust design of a compressor cascade. In the first formulation they minimize the expectation of the performance while in the second they minimize the variance of the performance with a constraint on the expectation.

Das [26] discussed the drawbacks of minimizing the expectation of the objective function. He argued that positive and negative deviations in the function value in the neighborhood of a target may cancel each other and this in turn may lead to convergence to a non-robust optimal design. Minimizing the variability function alone can lead to designs that are robust but not optimal and hence not desirable [26,27]. Therefore, it is desirable to optimize both the expectation and variance of the objective function. Robust design can be formulated as a multiobjective problem with the goal of simultaneously minimizing the mean and variance of the performance. More often than not there is a conflict between optimization of mean and variance and a trade off is required to choose optimal designs. The presence of multiple conflicting objectives in a problem leads to a set of optimal solutions, rather than a single solution. Such a solution set is referred to as a Pareto-optimal set in the optimization literature. Conventional methods simplify the bi-objective problem and obtain a combined objective function of the form $\mu(\mathbf{x})+W\sigma(\mathbf{x})$, where W is a user specified weighing parameter [28]. These methods are referred to as weighted sum (WS) methods [29]. The WS methods can only be used if the Pareto front is convex and fails to produce an even distribution of points from all parts of the Pareto set as W is varied [30].

Chen et al. [31] solved the bi-objective robust design problem from a utility perspective. They employ a compromise programming approach based on the Tchebycheff method. They further

[1]Corresponding author.

Contributed by the Design Automation Committee of ASME for publication in the JOURNAL OF MECHANICAL DESIGN. Manuscript received September 16, 2005; final manuscript received January 18, 2006. Review conducted by Zissimos P. Mourelatos.

improved their method by using a physical programming based approach where each objective was controlled with more flexibility. Genetic algorithms (GAs) are inherently well suited for solving multiobjective problems encountered in robust design, since they have the ability to find multiple Pareto-optimal solutions in a single run. Since GAs work with a population of solutions, it is easier to extend them to maintain high diversity in finding multiple Pareto-optimal solutions at each stage, while moving toward the true Pareto-optimal region [32]. In recent years several approaches have been proposed to solve multi-objective problems using GAs [33–35]. In the present study we employ the Non-dominated Sorting GA (NSGA-II) [36] in conjunction with surrogate models to efficiently solve multi-objective problems arising in robust design.

The robust design approach proposed here combines an efficient multiobjective optimization algorithm with a parametric geometry model, computational fluid dynamics (CFD) and surrogate models. The motivation behind this hybrid strategy is to ensure convergence close to the true Pareto front using a limited number of function evaluations. In the approach presented here, design of experiment (DOE) techniques are used to create an initial set of inner control and outer noise arrays. A parametric geometry model and grid generator is combined to generate meshes which are then used for CFD simulations. NSGA-II is then used in conjunction with a Gaussian stochastic process model to search the design space for Pareto-optimal solutions. A sequential search strategy is used to update the surrogate model as the optimization proceeds. The proposed method is applied to seek compressor fan blade sections that have robust performance in the presence of erosion. Detailed numerical studies are presented for robust geometric design of a typical compressor fan blade. The results obtained indicate that significant improvements in robustness can be achieved at a cost of a modest reduction in nominal performance.

The remainder of this paper is organized as follows. Section 2 describes the geometry modeling and parametrization method followed by the grid generation and CFD simulation details. The details of probabilistic performance analysis to understand the effect of erosion on the aerodynamic performance of the blade are presented in Sec. 3. In Sec. 4 we present the robust design methodology using NSGA-II and surrogate model. Finally, in Sec. 5 we present the numerical studies which is followed by the conclusions.

2 Modeling and Parametrization

Robust design methods require the definition of noise factors and control (design) factors in the system design. For the noise factors we need to develop a parametric model of the eroded compressor blade section. Erosion leads to blade surface deterioration and causes a depression in the original airfoil. Hence for modeling eroded geometries, an approach that can model local dents in the original airfoil shape is required. Hicks-Henne functions [37] provide a flexible tool to model local variation in the form of bumps. Erosion patterns observed in compressor fan blades can be very complex. A combination of piecewise cubic polynomial and Hicks-Henne function is used here to create a simplified model of the erosion patterns. The eroded compressor fan blade section is parametrized in terms of the location, depth, and the width of the eroded section. The Hicks-Henne function can be expressed as

$$b(x) = A[\sin(\pi x^{\log 0.5/\log t_1})]^{t_2} \quad 0 \leq x \leq 1 \tag{1}$$

Here, A is the maximum bump magnitude, t_1 is the position of the maximum of the bump, and t_2 controls the width of the bump. This provides us with three noise factors—location (t_1), width (t_2), and depth (A), for the robust design formulation.

The compressor blade geometry itself also needs to be parametrized to create a set of control factors. To parametrize the blade section geometry we use a linear combination of Hicks-Henne functions. Wu et al. [38] have presented and compared the efficacy of Hicks-Henne shape functions to other methods for modeling compressor blade sections. For the problem under consideration, we have used ten Hicks-Henne functions, five each for the upper and lower airfoil section, to parametrize the compressor fan blade. The Hicks-Henne shape functions can also be expressed as

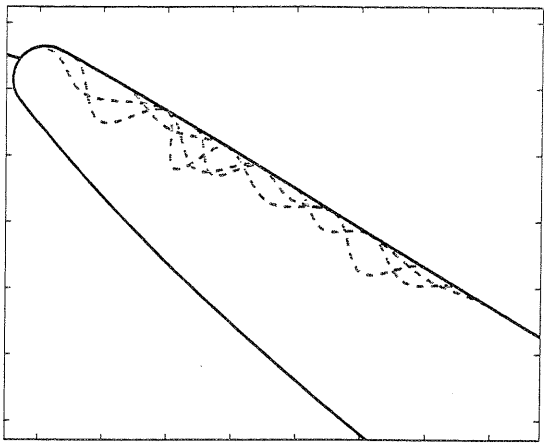

Fig. 1 Blades with variations in noise factors

$$b_i(x) = \sin^4(\pi x^{m_i}) \quad m_i = \ln(0.5)/\ln(x_{M_i}) \quad \text{where } i = 1,2,\ldots,n \tag{2}$$

where x is the normalized chordwise coordinate from leading edge to the trailing edge ($0 \leq x \leq 1$), x_{M_i} are preselected values corresponding to the location of the maxima, and n is the number of Hicks-Henne functions used. In the present study, the locations of x_{M_i} for $i=1,2,\ldots,5$ are chosen to be $0.5[1-\cos(\delta_i)]$, where $\delta_i = \pi i/6$. This choice of x_{M_i} ensures that the distribution is denser near the leading edge and trailing edge, where the curvature is high. These shape functions are added to a typical Rolls-Royce compressor fan blade section to obtain new shapes. The amplitudes of these shape functions are used as design variables. Hence, for our robust design study we have ten design variables which can be treated as the control factors and three noise factors representing the erosion pattern. Figures 1 and 2 show the variations in geometry caused by changing the noise factors and control factors, respectively.

The geometry model discussed above is combined with the Rolls-Royce propriety code PADRAM, a parametric design and meshing routine employed for automating the geometry creation and grid generation process [39]. PADRAM makes use of both transfinite interpolation and elliptic grid generation to generate hybrid C-O-H meshes. An orthogonal body fitted O mesh is used

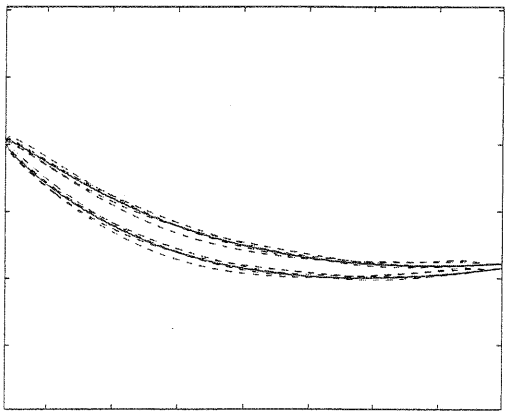

Fig. 2 Blades with variations in control factors

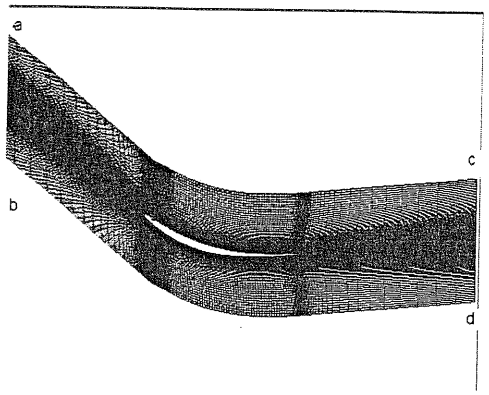

Fig. 3 A typical C-O-H mesh used for CFD analysis

to capture the viscous region of the airfoil whilst an H mesh is used near the boundary where stretched cells are required, for example, in the wake region. After grid refinement studies we select a mesh of the order of 28,000 cells in two dimensions.

In Fig. 3 *abdc* is the CFD domain where the boundary *ab* is the inlet and the boundary *cd* is the outlet. Figure 4 shows the pressure contour plot of compressor blade with erosion. A nonlinear, unstructured viscous flow solver HYDRA is used for the CFD simulation [40]. It solves the Reynolds averaged steady Navier-Stokes (RANS) equations with the Spalart-Allmaras turbulence model. To accelerate convergence to steady-state HYDRA employs a multigrid algorithm with preconditioning [41]. A four level multigrid is used for the present simulations. The inlet boundary conditions for the CFD analysis are total temperature =290 K, total pressure=63,400 Pa, whirl angle=−37.28 deg, and the outlet boundary condition is static pressure=52,000 Pa. An initial uniform flow condition with density=0.7675 kg/m^3, velocity=0, and Pressure=66,932 Pa is considered. The converged CFD solution is used to calculate the pressure loss at the nominal geometry. The equation for the pressure loss is

$$\text{Loss} = \frac{P_{\text{inlet}} - P_{\text{exit}}}{P_{\text{inlet}}} \times 100 \tag{3}$$

where P_{inlet} is the total pressure at the inlet and P_{exit} is the total pressure at the exit.

3 Probabilistic Performance Analysis

In the following we present a probabilistic approach based on surrogate modeling to analyze the effect of erosion parameters on the aerodynamic performance of compressor fan blades. We employ a Gaussian stochastic process model as a cheap surrogate to the high-fidelity CFD code. To understand the effect of the noise parameters on design performance a main effect study is first performed. The quality of the surrogate model is verified prior to employing it for Monte Carlo simulation (MCS) based probabilistic analysis. The studies suggest up to 6% degradation in pressure loss.

3.1 Surrogate Modeling. The computational cost associated with high-fidelity simulation rules out the direct application of the MCS technique to probabilistic analysis. Surrogate modeling uses the basic idea of analyzing an initial set of design points to generate data which can be used to construct computationally cheap approximations of the original high-fidelity model. The CFD simulator used for high-fidelity analysis in this study can be represented by the functional relationship $y=f(\mathbf{x})$, where $\mathbf{x}$ is the vector of inputs to the simulation code and y is the output. The objective is to construct an approximate model $\hat{y}=\hat{f}(\mathbf{x},\boldsymbol{\alpha})\approx f(\mathbf{x})$, that is computationally cheaper to evaluate. $\boldsymbol{\alpha}$ is a vector of undetermined hyperparameters which is estimated using the input-output data set $\{\mathbf{x}^{(i)},y^{(i)}\}, i=1,2,\ldots,n$. In general, surrogate modeling involves the following steps: (1) data generation, (2) model structure selection, (3) parameter estimation, and (4) model validation. A detailed exposition of these steps can be found in Ref.

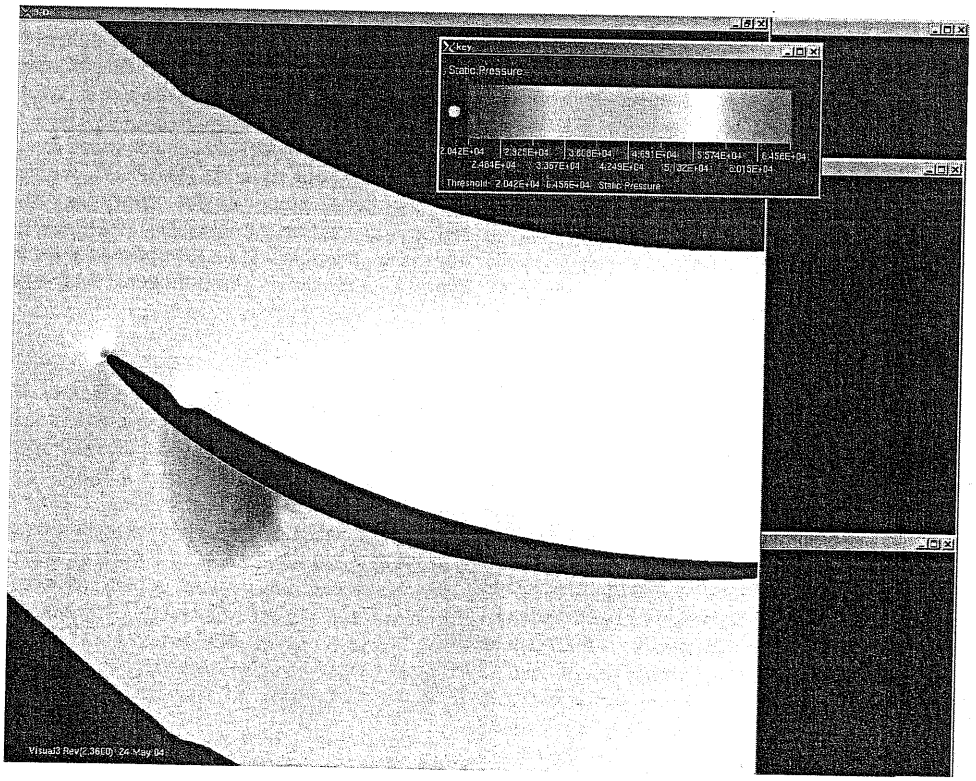

Fig. 4 CFD static pressure plot

[42].

In the present study we use a Gaussian stochastic process model as a surrogate to the high-fidelity CFD simulation code. This approach was originally developed in the field of geostatistics (where this approach is referred to as Kriging) and has been in use since the early 1960s [43]. It is also widely used in the neural network community where it is referred to as Gaussian process regression [44,45]. The model structure typically used in Gaussian stochastic process modeling can be expressed as

$$Y(\mathbf{x}) = g(\mathbf{x}) + Z(\mathbf{x}) \tag{4}$$

The above model is a combination of a global model ($g(\mathbf{x})$) and a local model ($Z(\mathbf{x})$). $g(\mathbf{x})$ is usually a linear or quadratic polynomial function, however, a constant $g(\mathbf{x})=\beta$ is often found to be sufficient for modeling complex functions. $Z(\mathbf{x})$ is a Gaussian random function with zero mean and nonzero covariance and is used to model the local deviations from the global model, i.e.,

$$\text{Mean}(Z(\mathbf{x})) = 0 \text{ and } \text{Cov}(Z(\mathbf{x}),Z(\mathbf{x}')) = \Gamma(\mathbf{x},\mathbf{x}') = \sigma_z^2 R(\mathbf{x},\mathbf{x}') \tag{5}$$

In other words, the observed outputs of the simulation code $\mathbf{y} = \{y^{(1)}, y^{(2)}, \ldots, y^{(n)}\}$ are assumed to be realizations of a Gaussian random field with mean β and covariance Γ. Here $R(.,.)$ is a parametrized correlation function that can be tuned to the training data set and σ_z^2 is the so-called process variance.

A commonly used choice of covariance function is the stationary family which obeys the product correlation rule [46],

$$R(\mathbf{x}^{(1)},\mathbf{x}^{(2)}) = \prod_{j=1}^{p} \exp(-\theta_j |\mathbf{x}_j^{(1)} - \mathbf{x}_j^{(2)}|^{\gamma_j}) \tag{6}$$

where $\theta_j \geq 0$ and $1 < \gamma_j \leq 2$ are the hyperparameters. In theory, the choice of an optimal covariance function is data dependent. However, in practice it has been found that the parametrized covariance function in Eq. (6) offers sufficient flexibility for modeling smooth as well as nonlinear functions [47]. If a Gaussian process prior over functions is used, the posterior process is also Gaussian. Hence using standard results from Bayesian inferencing, the posterior mean and covariance can be stated as

$$\hat{y}(\mathbf{x}) = \beta + \boldsymbol{\tau}(\mathbf{x})^T \mathbf{R}^{-1}(\mathbf{y} - \mathbf{1}\beta) \tag{7}$$

and

$$C(\mathbf{x},\mathbf{x}') = \sigma_z^2 (R(\mathbf{x},\mathbf{x}') - \boldsymbol{\tau}(\mathbf{x})^T \mathbf{R}^{-1} \boldsymbol{\tau}(\mathbf{x}')) \tag{8}$$

Here $\mathbf{R}$ is the correlation matrix whose ijth element is calculated as $R(\mathbf{x}^{(i)},\mathbf{x}^{(j)})$, $\boldsymbol{\tau}(\mathbf{x}) = \{R(\mathbf{x},\mathbf{x}^{(1)}), R(\mathbf{x},\mathbf{x}^{(2)}), \ldots, R(\mathbf{x},\mathbf{x}^{(n)})\}^T \in \mathbb{R}^n$ and $\mathbf{1} = \{1,1,\ldots,1\}^T \in \mathbb{R}^n$. The hyperparameters $\boldsymbol{\theta}, \beta, \sigma_z^2$ are computed from the training data set via maximum likelihood estimation, which involves solving the following optimization problem

$$\{\boldsymbol{\theta},\beta,\sigma_z^2\} = \arg \max_{\{\boldsymbol{\theta},\beta,\sigma_z^2\}} \frac{1}{2}\left[n \ln(2\pi) + n \ln \sigma_z^2 + \ln|\mathbf{R}| + \frac{1}{\sigma_z^2}(\mathbf{y} - \mathbf{1}\beta)^T \mathbf{R}^{-1} (\mathbf{y} - \mathbf{1}\beta) \right] \tag{9}$$

In the numerical studies presented here, we use a hybrid GA to solve the above optimization problem.

It may be noted from Eqs. (7) and (8) that the Gaussian stochastic process modeling approach finally leads to an approximation of the high-fidelity computational model as a multidimensional Gaussian random field. The posterior variance $\sigma^2(\mathbf{x}) = C(\mathbf{x},\mathbf{x})$ can be interpreted as an estimate of the uncertainty involved in predicting the output at any new points using the given finite data set. One key advantage of this approach is that the user can get an estimate of the prediction error, which can be exploited in optimization procedures to sequentially update the surrogate model and hence improve its predictive capability [48,42].

Once the surrogate model is constructed, it can be employed to efficiently compute the statistics of the response quantities. To illustrate, consider the case when the input vector $\mathbf{x}$ is Gaussian with the specified joint probability density function $\mathcal{P}(\mathbf{x})$ and it is desired to compute the mean of the output quantity $y(\mathbf{x})$. Since the surrogate model for $y(\mathbf{x})$ is a Gaussian random field, it follows that the approximation for the mean of $y(\mathbf{x})$ is a Gaussian random variable [42], i.e.,

$$K = \int_{\mathcal{E}} y(\mathbf{x}) \mathcal{P}(\mathbf{x}) d\mathbf{x} \sim \mathcal{N}(\langle K \rangle, \sigma_K^2) \tag{10}$$

where

$$\langle K \rangle = \int_{\mathcal{E}} \hat{y}(\mathbf{x}) \mathcal{P}(\mathbf{x}) d\mathbf{x} \quad \sigma_K^2 = \int_{\mathcal{E}} \int_{\mathcal{E}} C(\mathbf{x},\mathbf{x}') \mathcal{P}(\mathbf{x}) \mathcal{P}(\mathbf{x}') d\mathbf{x} d\mathbf{x}' \tag{11}$$

and $\mathcal{E}$ is the support region of $\mathcal{P}(\mathbf{x})$. Here $\langle K \rangle$ can be interpreted as an estimate of $\langle y(\mathbf{x}) \rangle$, while σ_K^2 is a probabilistic error bar.

Note that the multidimensional integrals in Eq. (11) can be evaluated analytically only for special cases; for example, when the input variables are Gaussian random variables and the correlation function $R(\mathbf{x},\mathbf{x}')$ obeys the product correlation rule. Fortunately, since predicting the output at a new point $\mathbf{x}$ using the surrogate is computationally very cheap (only matrix vector and vector vector products are involved), simulation techniques can be readily applied to compute $\langle K \rangle$ and σ_K^2 when analytical expressions cannot be derived.

One of the limitations of nonparametric techniques like Gaussian stochastic process modeling, as compared to parametric models, is that the underlying input-output relationship is not available in a readily interpretable form. Hence, it is not straightforward to understand the effects of each input variable on the output performance. In order to understand the underlying functional relationship, the effect of each input parameter has to be isolated. The main effect of an input can be evaluated by integrating out the effect of the other input variables [49,50]. The main effect of the ith variable can be expressed as

$$\mu(x_i) = \frac{1}{V} \int y(\mathbf{x}) \prod_{h \neq i} dx_h \tag{12}$$

In most cases it is cumbersome to evaluate the above integral analytically. However, a numerical approximation can be obtained by performing a summation over a set of m discrete points $[\mathbf{x}^{(1)}, \mathbf{x}^{(2)}, \ldots, \mathbf{x}^{(m)}]$. The m points can be generated by using DOE techniques like random MCS or Latin hypercube sampling. Note that since the Gaussian stochastic process model also provides the posterior variance, error bars on the main effects can be readily computed [50]. More precise methods for the global sensitivity analysis have been discussed in Ref. [51].

3.2 Probabilistic Studies. To construct a Gaussian process surrogate model, we carry out a 90 point LP_τ DOE survey [52] over the values of the erosion parameters [location, width, height]. The parameters of the eroded geometry are specified by upper and lower bounds. The automated grid generator and CFD simulator are run to evaluate the pressure loss at each design point. The scatter plot of the normalized values of pressure loss are shown in Fig. 5. It can be observed that the pressure loss for most of the eroded geometries have deteriorated. A few geometries with subtle shape changes had a slightly improved performance as compared to the nominal geometry.

The quality of the surrogate model can be assessed by a leave-one-out type cross-validation procedure. This method involves leaving the ith training point out and computing the posterior mean at the point $(\hat{y}_{-i}(\mathbf{x}))$. Standardized cross-validated residual

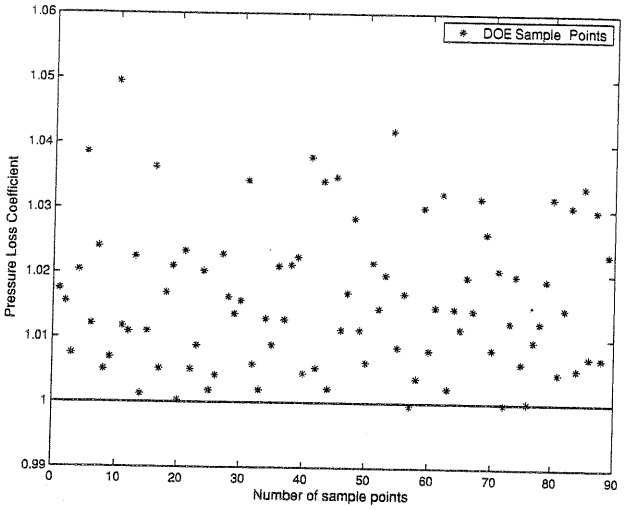

Fig. 5 The scatter plot of pressure loss using the training data set

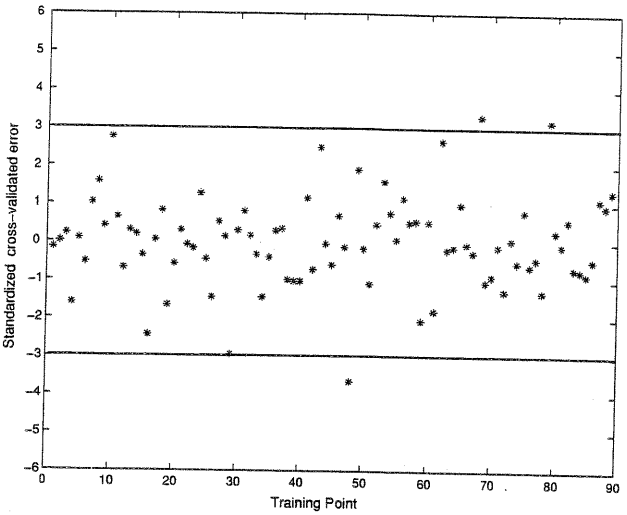

Fig. 7 $SCVR_i$ values using leave-one-out validation

(SCVR) is another measure of model quality and is discussed in detail in Ref. [46]. Figure 6 shows the plot of posterior mean and Fig. 7 shows the SCVR values predicted by the leave-one-out method. The regression coefficient for a linear model fit to the leave-one-out results is R^2=0.954. It can also be observed that most of the $SCVR_i$ in Fig. 7 lie within the range $[-3\sigma, +3\sigma]$ and hence the error bars computed using the surrogate are reasonably tight.

Having established the quality of the surrogate model we use it to study the effect of erosion parameters on the blade at modest computational cost. A 10,000 point MCS is run on the surrogate model to generate the probability distribution of the pressure loss assuming a uniform distribution for the erosion parameters [location, width, height]. The histogram for the pressure loss evaluated using MCS is shown in Fig. 8. The MCS using the surrogate model takes less than 4 s for carrying out 10,000 evaluations on an Intel® Xeon™ CPU 3.06 GHz dual processor machine. This shows substantial savings in computational time, as compared to using the high-fidelity CFD model for probabilistic studies.

The values of the hyperparameter $\theta=[\theta_{location}, \theta_{width}, \theta_{height}]$ can be used to understand the relative importance of the erosion parameters on the pressure loss. The higher the value of the hyperparameter for a particular design variable, the more that design variable affects the output performance [42]. We found the θ values corresponding to location, width, and height to be 1.413, 0.227, and 1.623, respectively. Since there was no significant difference in these values, no insight into the relative importance of the input variables could be made. Main effect studies were carried out by numerically integrating out the effect of other variables. The main effect plots for [location, width, height] are shown in Figs. 9–11, respectively. The main effect plots for location and width of the erosion are relatively flat as compared to the main effect plot for height. This suggests that height of the erosion is the most influential input variable. The main effects plots also suggest that there is an approximately linear relationship between pressure loss and the location and width of the erosion. However, a relatively nonlinear underlying relationship between the height of the erosion and pressure loss is predicted. The probabilistic analysis suggested up to 6% degradation in pressure loss which emphasizes the need for blades which are robust against erosion. Since no one variable shows less effect on the performance as compared to the other two variables, we consider all of them for the robust design studies.

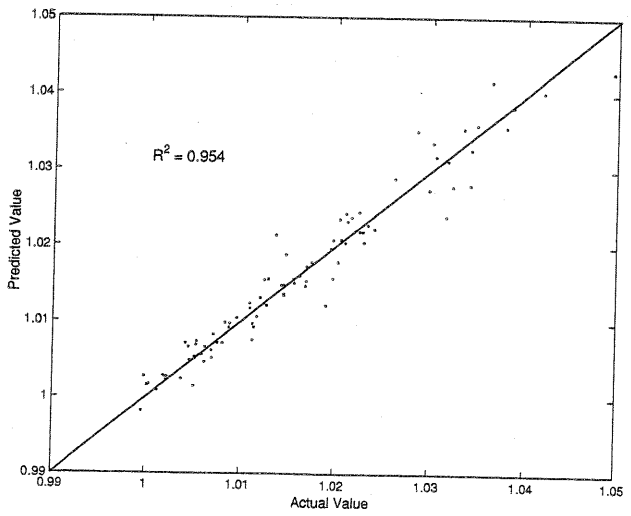

Fig. 6 Predicted posterior mean versus observed values (R^2 =0.954)

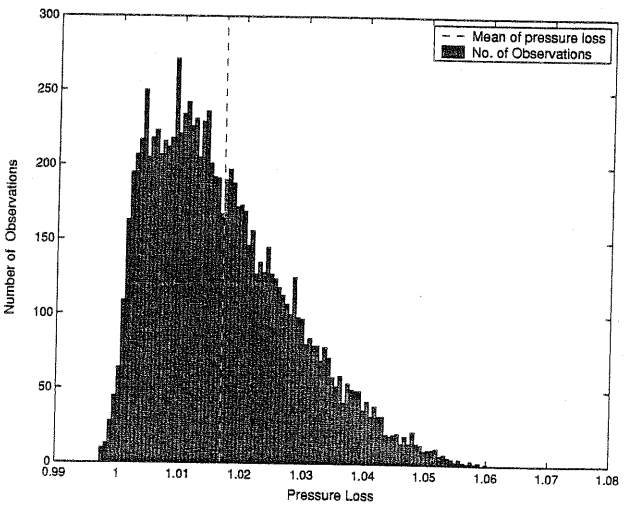

Fig. 8 Probability distribution of the pressure loss using MCS

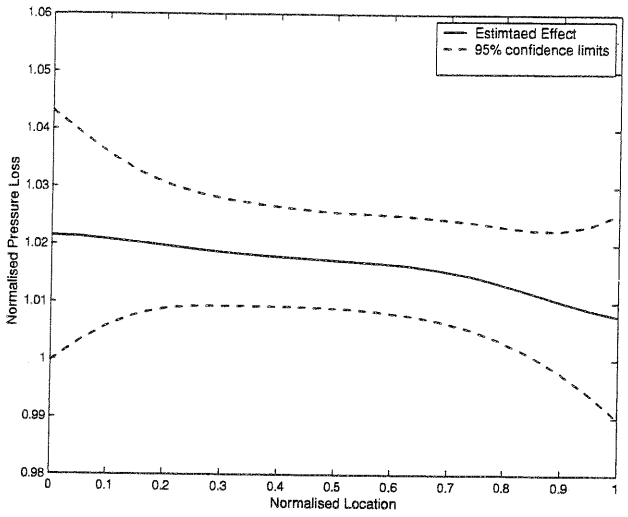

Fig. 9 Main effect plot for location

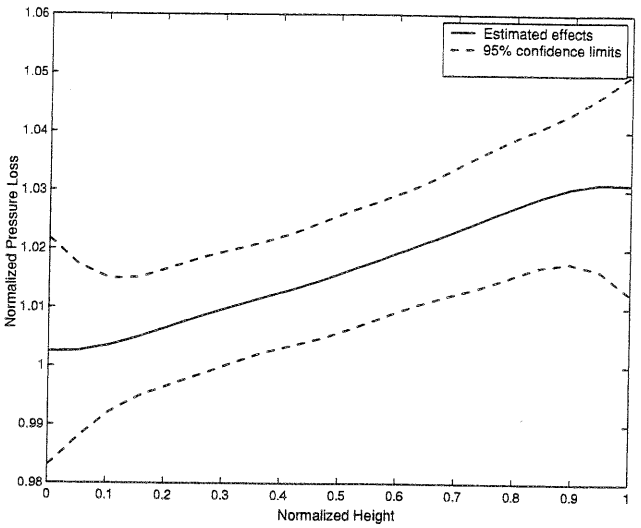

Fig. 11 Main effect plot for height

4 Robust Design Methodology

Robust design can be formulated as a multiobjective problem with the goal of simultaneously minimizing the mean and standard deviation of the performance, i.e.,

$$\text{Minimize: } \mu = \frac{1}{k}\sum_{i=1}^{k} \text{Pl}_i \text{ and}$$

$$\text{Minimize: } \sigma = \sqrt{\frac{1}{k-1}\sum_{i=1}^{k} (\text{Pl}_i - \mu)^2} \quad i = 1,2,\ldots,k \quad (13)$$

where Pl is the pressure loss and k is the number of eroded compressor blade types used for representing the sample space. The presence of multiple objectives in a problem leads to a set of Pareto optimal solutions, rather than a single solution. Each point in the set is optimal in the sense that no improvement can be achieved in one objective without worsening the other objective. In the absence of further information about the relative importance of the objectives, it is not possible to decide which design is better than the rest. Hence, it is important to find as many Pareto-optimal solutions as possible for the benefit of the designer.

Classical optimization methods suggest converting the multiple objective optimization problem to a single objective optimization problem emphasizing one particular Pareto-optimal solution at a time. Such methods prove to be computationally expensive and do not ensure convergence to true optimal Pareto sets in nonconvex problems [53,54]. In contrast, GAs are inherently suited for multiobjective problems as they have the ability to find multiple Pareto-optimal solutions in one simulation run. Since GAs work with a population of solutions, it is easier to extend them to maintain high diversity in finding multiple Pareto-optimal solutions at each stage, while moving toward the true Pareto-optimal region [32].

In recent years several approaches have been proposed to solve multiobjective problems using GAs [33,55,34,35]. The elitism based NSGA-II proposed by Deb et al. [36] is employed here to seek the Pareto-optimal front. The NSGA-II method is fast since it has a computational complexity of $\mathcal{O}(MN^2)$ (where M is the number of objectives and N is the population size) when compared to other nondominated GAs with computational complexity $\mathcal{O}(MN^3)$. The NSGA-II method also uses elitism to enhance the performance of the GA and prevent the loss of good solutions once they are found. Traditional GA methods ensure diversity in a population by relying on the concept of sharing. In such methods it is necessary to specify the sharing parameter (σ_{share}) beforehand by the user. The performance of sharing functions in ensuring diversity is dependent upon the choice of σ_{share}. In practice it is not very obvious how to select the best value of σ_{share}. In NSGA-II the sharing function approach is replaced by a crowded comparison approach. The crowded comparison approach has a lower computational complexity and eliminates any user defined parameter for maintaining diversity among population members. In this study NSGA-II is employed in conjunction with surrogate models to identify the Pareto-optimal front to seek robust designs.

In the robust design method employed in this study we first select the design space and use DOE techniques to rationally choose a set of compressor fan blade sections as m initial candidate points. Subsequently a second level of DOE is run to suggest n different erosion geometries on each candidate compressor fan blade section. This is very similar to the inner control factor array of m points and noise factor array of n points used in Taguchi's system design. The eroded compressor blades are modeled using the parametrization method discussed in Sec. 1. PADRAM is used to produce high quality hybrid meshes and the multigrid RANS solver HYDRA with Spalart Allmaras turbulence model is used for CFD simulations to calculate the total pressure loss over the compressor blade section at each of the $m \times n$ points. The mean and standard deviation of the total pressure loss (over n erosion types settings) is calculated for all the m blade sections.

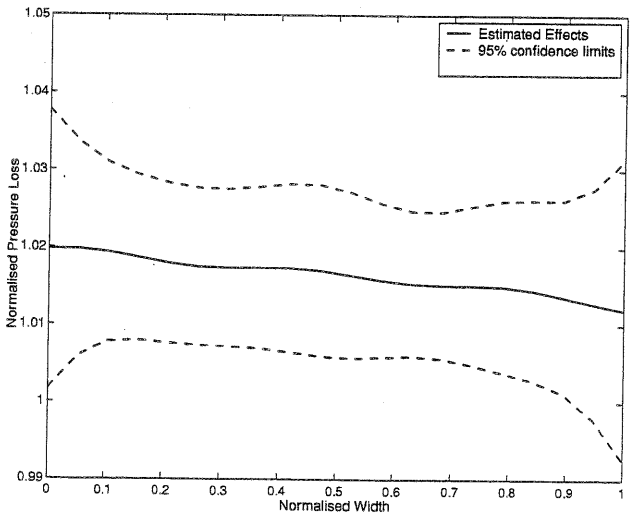

Fig. 10 Main effect plot for width

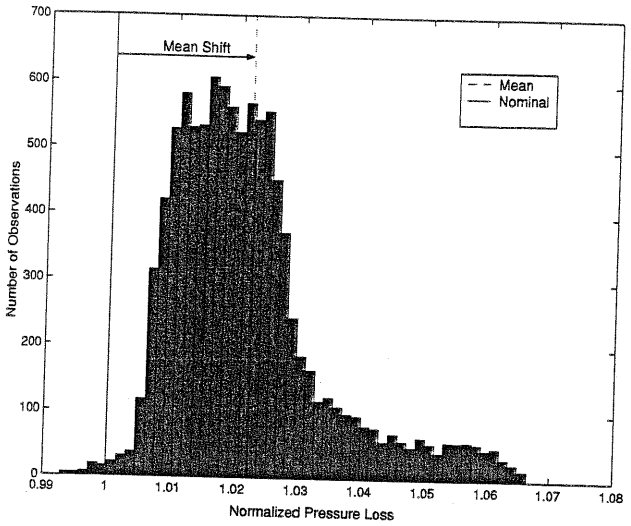

Fig. 15 Histogram of pressure loss in presence of erosion

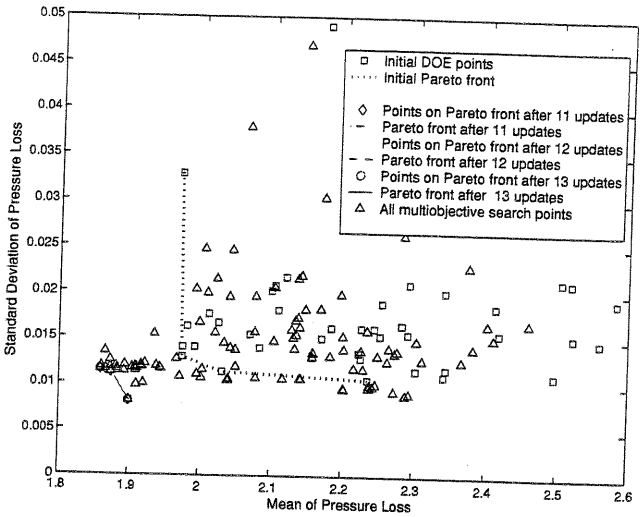

Fig. 16 Plot of the initial data set with the initial Pareto front and all the search points. The plot also shows the last three Pareto fronts after which the search was terminated. Note that the 11th, 12th, and 13th Pareto fronts are the same and overlap, hence they are not distinguishable in the plot.

5.2 Robust Design Studies. The robust design method discussed earlier is applied to a typical Rolls-Royce compressor fan blade section. An LP_τ based DOE is employed to create an initial control factor set of m (m=50) compressor fan blade shapes. This is followed by another set of LP_τ based DOE to create n (n=15) types of erosion on each of the m blade shapes. The noise factors—location (t_1), width (t_2), and depth (A) are represented by a uniform distribution. Figure 1 shows some of the shapes generated. PADRAM is employed for generating high quality CFD meshes and a multigrid RANS based CFD simulation is performed at the $m \times n$ candidates points to evaluate the mean and variance of the pressure losses corresponding to the m designs. NSGA-II is used in conjunction with Gaussian stochastic process models for the mean and variance of the loss coefficient to seek Pareto optimal solutions. After each search iteration 10 points are selected on the Pareto front obtained using the surrogate models using a low crowding algorithm. Exact runs of the CFD code are carried out at these points and the resulting data are used to update the baseline surrogate models for the mean and variance.

The NSGA-II algorithm with the update method is employed for 13 updates to find the optimal robust design set. The search is terminated when there is no further improvement in the Pareto front. Figure 16 shows the convergence of the Pareto fronts. It can be observed from Fig. 16 that the last three Pareto fronts are same, and hence the search was terminated. It should be noted that this termination criterion does not ensure convergence to the true Pareto front. However, our primary objective is to seek design improvements on a limited computational budget and this has been achieved. Figure 16 shows the initial data set with the initial Pareto front (dotted line). The solid line shows the final Pareto front. It can be noted from Fig. 16 that significant improvement in the Pareto front has been achieved.

A 50 point LP_τ based DOE with noise factors—location (t_1), width (t_2), and depth (A) is executed for a selected geometry on the final Pareto front. The data are used to train a surrogate model, which is further used for an MCS. An MCS of 10,000 runs is executed for the selected blade geometry and the histograms of the pressure loss are generated. Figure 17 shows the robust geometry as compared to the baseline geometry. Figure 18 shows histograms of pressure loss for the robust geometry.

We compare the performance of the geometry which was optimized for pressure loss coefficient using the deterministic method with the selected robust geometry. Figure 19 shows the histograms for both geometries with nominal pressure loss coefficient and the mean of the pressure loss coefficient in the presence of erosion. The histogram of the robust geometry shows less variability in pressure loss coefficient as compared to the design obtained using a deterministic approach. There is considerably lower shift in the mean performance of 0.7% from the nominal performance for the robust blade geometry as compared to almost 2% for the deterministic optimal blade geometry. It can be observed that low variability has been achieved in the robust design at the expense of a marginal reduction in the mean performance. The worst case performance of the robust blade geometry is also considerably better than the deterministic optimal blade geometry.

6 Conclusions

In this paper we have presented an efficient and fast genetic algorithm based robust design methodology. A novel parametrization method was developed to model eroded compressor fan blade sections. A LP_τ based DOE technique was used to construct an initial inner control array and outer noise array. A parametric grid generation routine was used to automate geometry creation and grid generation to construct high quality CFD meshes which were then solved using a RANS code. Gaussian stochastic process models were used as computational surrogates to the high-fidelity

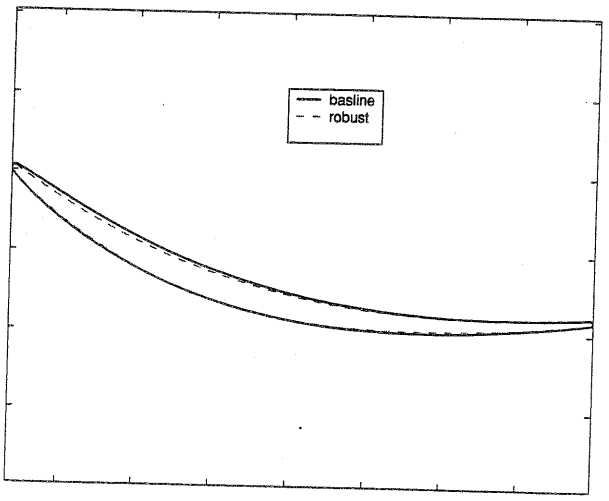

Fig. 17 Shape of robust and baseline geometry

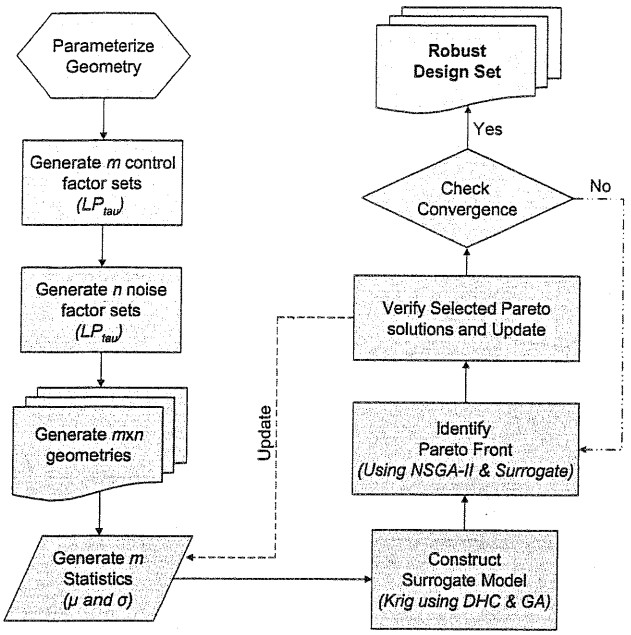

Fig. 12 Flowchart for robust design methodology

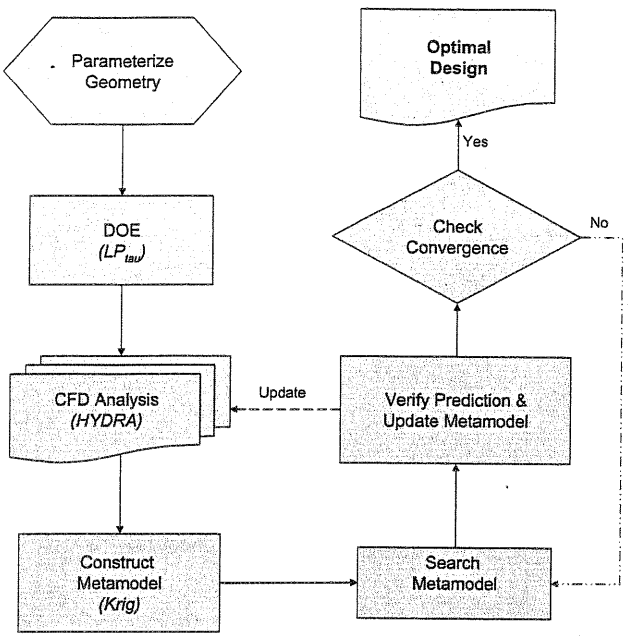

Fig. 13 Flowchart for deterministic surrogate-assisted design optimization

Unlike conventional robust design procedures we do not limit ourselves to just searching the initial design space. A Gaussian stochastic process model is employed to generate a computationally less expensive surrogate to predict the mean and standard deviation of the total pressure loss. The hyperparameters $\theta, \beta, \sigma_z^2$ of the surrogate model are estimated via maximum likelihood estimation. NSGA-II is then used to search the entire design space to obtain Pareto-optimal solutions. A low-crowding algorithm is used to select points for CFD evaluations and updating the surrogate models. This step essentially involves calculating the Euclidian distance between the candidate points suggested by the surrogate-assisted optimizer to the existing set of points. Only the first ten points with maximum distance are chosen due to computational cost considerations. As each CFD simulation takes 32 min on a Intel Xeon CPU 3.06 GHz dual processor machine, one update cycle (10 runs with 15 runs in the inner loop to compute the statistics over the noise variables) takes approximately 4800 min (80 h) on a single machine. The surrogate model is then updated at the suggested points and this process is performed iteratively until some convergence criteria is satisfied or the specified computational budget is exhausted. In the present study, the process is terminated if for more than two update iterations, there is no improvement in Pareto front as compared to the previous best Pareto front. The designer can subsequently use the resulting optimal design set to trade off between mean performance and variance to obtain robust designs. The proposed methodology is outlined in the flowchart in Fig. 12.

5 Numerical Studies and Results

5.1 Deterministic Design. To provide a benchmark against which the results of a multiobjective robust design search can be compared, we begin with a traditional deterministic optimization approach. Deterministic design methods seek to optimize the nominal performance of the system, i.e., optimize blade geometries for low pressure loss coefficients. An LP_τ based DOE is employed to generate an initial set of training points containing different blade geometries whose performances are evaluated using the CFD code. The initial data set is subsequently used to construct a baseline surrogate model which is then used in lieu of the CFD simulator during optimization. During the optimization iterations, the surrogate models are updated in a sequential fashion to improve its accuracy. The approach employed is illustrated by the flowchart in Fig. 13.

Once the optimal blade is found we then analyze its behavior in the presence of erosion. A probabilistic analysis, similar to the study performed earlier, is employed to study the deviation in coefficient of pressure loss for the resulting design. A 50 point LP_τ DOE survey is performed over the values of the erosion parameters [location, width, height] and CFD calculations using HYDRA are executed at these points. The initial data set is used to train a Gaussian stochastic process model. An MCS of 10,000 runs is employed to obtain the statistics of the blade performance. Figures 14 and 15 show the deterministic optimal blade and histogram of the pressure loss coefficient obtained using MCS.

As expected, the optimal blade obtained (see Fig. 14) from the deterministic optimization has good nominal performance but the performance deteriorates significantly in the presence of erosion. It can be observed from Fig. 15 that there is almost 2% shift in the mean pressure loss coefficient from the nominal pressure loss coefficient.

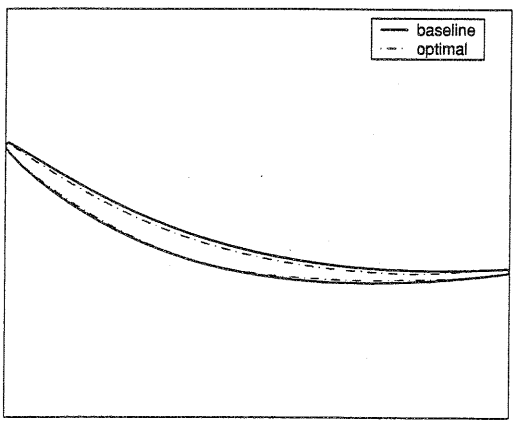

Fig. 14 Baseline and optimal blade shapes

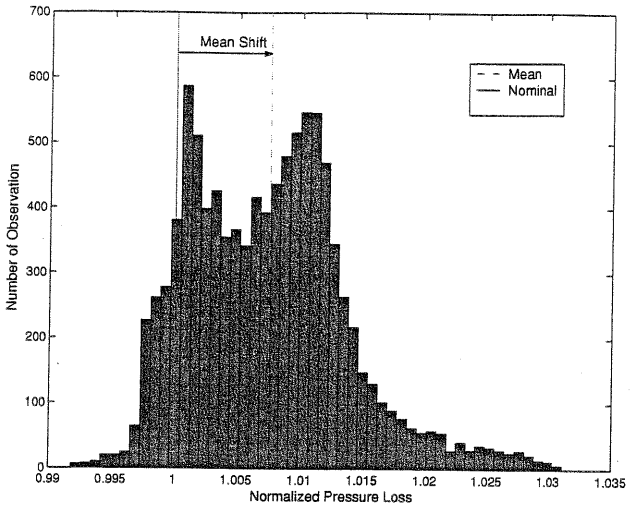

Fig. 18 Histogram of pressure loss of the robust geometry

CFD simulations in order to ensure convergence close to the true Pareto front using a limited number of exact function evaluations.

The robust design problem was formulated as a multiobjective problem. An elitism based non-dominated sorting genetic algorithm was employed in conjunction with the surrogate model to search the design space. A Pareto-optimal set was identified for trade off between the mean and standard deviation of the pressure loss. The efficiency of the proposed solutions would depend on the quality of the surrogate model used. The Pareto-optimal set suggested by the NSGA-II, using the surrogate model, was verified using CFD simulations and few points were selected from the final Pareto front for further analysis and updating the surrogate models. An MCS based on surrogate models was executed for the selected blades and the results were found to be considerably better and robust than the design obtained using a deterministic optimization approach. The method presented can be employed to seek robust optimal sets which can be presented to the designers to find compressor blade designs that are robust to erosion processes.

Acknowledgment

This work was supported by the University Technology Partnership for Design, a collaboration between Rolls-Royce Plc., BAE Systems and the Universities of Sheffield, Cambridge and Southampton.

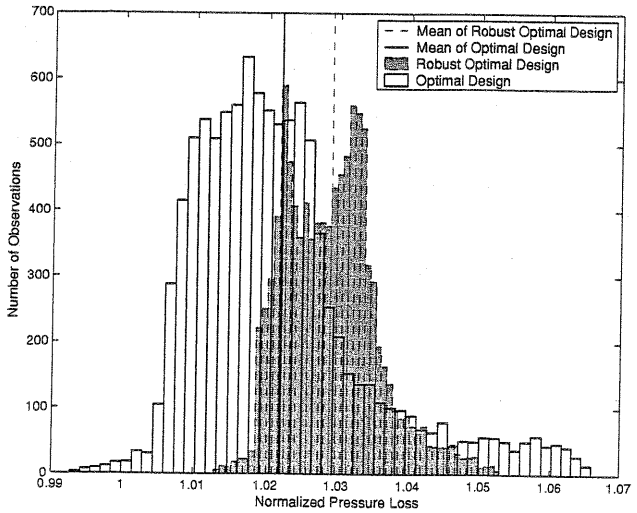

Fig. 19 Histograms of robust and deterministic optimal geometries

References

[1] Metwally, M., Tabakoff, W., and Hamed, A., 1995, "Blade Erosion in Automotive Gas Turbine Engine," J. Eng. Gas Turbines Power, **117**, pp. 213–219.
[2] Hamed, A., Tabakoff, W., and Sing, D., 1998, "Modeling of Compressor Performance Deterioration Due to Erosion," Int. J. Rotating Mach., **4**, pp. 243–248.
[3] Roberts, W. B., 1984, "Axial Compressor Performance Restoration by Blade Profile Control," AIAA-84-GT-232, ASME.
[4] Kumar, A., Nair, P. B., Keane, A. J., and Shahpar, S., 2005, "Probabilistic Performance Analysis of Eroded Compressor Fan Blades," ASME Power PWR2005-50070.
[5] Zang, T. A., Hemsch, M. J., Hilburger, M. W., Kenny, S. P., Luckring, J. M., Maghami, P., Padula, S. L., and Stroud, W. F., 2002, "Needs and Opportunities for Uncertainty-Based Multidisciplinary Design Methods for Aerospace Vehicles," Technical Report NASA/TM-2002-211462, NASA Langley Research Center, Hampton, VA.
[6] Phadke, M. S., 1989, *Quality Engineering using Robust Design*, Prentice Hall, Englewood Cliffs, NJ.
[7] Taguchi, G., and Wu, Y., 1980, *Introduction to Off-Line Quality Control*, Central Japan Quality Control Association, Nagoya, Japan.
[8] Taguchi, G., 1986, *Introduction to Quality Engineering*, UNIPUB/Krauss International, New York.
[9] Nair, V. N., 1992, "Taguchi's Parameter Design: A Panel Discussion," Technometrics, **34**, pp. 127–161.
[10] Trosset, M. W., 1996, "Taguchi and Robust Design," Technical Report No. 96–31, Houston, TX.
[11] Box, G. E. P., 1988, "Signal-to-Noise Ratios, Performance Criteria, and Transformations (with discussions)," Technometrics, **30**(1), pp. 1–17.
[12] Trosset, M. W., Alexandrov, N. M., and Watson, L. T., 2003, "New Methods for Robust Design Using Computer Simulations," *American Statistical Association, 2003, Proceedings of the Section on Physical and Engineering Science.*
[13] Welch, W. J., Yu, T. K., Kang, S. M., and Sacks, J., 1990, "Computer Experiments for Quality Control," J. Quality Technol., **22**, pp. 15–22.
[14] Welch, W. J., and Sacks, J., 1991, "A System for Quality Improvement via Computer Experiments," Commun. Stat: Theory Meth., **20**, pp. 477–495.
[15] Ben-Tal, A., and Nemirovski, A., 1997, "Robust Truss Topology Design via Semidefinite Programming," SIAM J. Optim., **7**, pp. 991–1016.
[16] Gunawan, S., and Azarm, S., 2004, "Non-gradient Based Parameter Sensitivity Estimation of Single Objective Robust Design Optimization," ASME J. Mech. Des., **126**, pp. 395–402.
[17] Huyse, L., and Lewis, R., 2001, "Aerodynamic Shape Optimization of Two-Dimensional Airfoils Under Uncertain Operating Conditions," Technical Report NASA/CR-2001-210648, Langley Research Center, Hampton, VA.
[18] Li, W., Huyse, L., and Padula, S., 2002, "Robust Airfoil Optimization to Achieve Drag Reduction Over a Range of Mach Numbers," Struct. Multidiscip. Optim., **24**, pp. 38–50.
[19] Tsutsui, S., and Ghosh, A., 1997, "Genetic Algorithms with a Robust Solution Searching Scheme," IEEE Trans. Evol. Comput., **1**, pp. 201–208.
[20] Tsutsui, S., Ghosh, A., and Fujimoto, Y., 1996, "A Robust Solution Searching Scheme in Genetic Search," in *Proceedings of Parallel Problem Solving in Nature*, pp. 543–552.
[21] Huyse, L., 2001, "Solving Problems of Optimization Under Uncertainty as Statistical Decision Problem," AIAA Pap., 2001–1519.
[22] Parkinson, D. B., 1997, "Robust Design by Variability Optimization," Qual. Reliab. Eng. Int, **13**, pp. 97–102.
[23] Al-Widyan, K., and Angeles, J., 2005, "A Model-Based Formulation of Robust Design," ASME J. Mech. Des., **127**, pp. 388–396.
[24] Jin, Y., and Branke, J., 2005, "Evolutionary Optimization in Uncertain Environments: A Survey," IEEE Trans. Evol. Comput., **9**(3), pp. 303–317.
[25] Garzon, V. E., 2003, "Probabilistic Aerothermal Design of Compressor Airfoils," Ph.D. thesis, Massachusetts Institute of Technology.
[26] Das, I., 2000, "Robustness Optimization for Constrained Nonlinear Programming Problems," Eng. Optimiz., **32**(5), pp. 585–618.
[27] Jin, Y., and Branke, J., 2003, "Tradeoff Between Performance and Robustness: An Evolutionary Multiobjective Approach," *Evolutionary Multi-Criterion Optimization*, Springer, Berlin, LNCS 2632.
[28] Chen, W., Allen, J. K., Tsui, K.-L., and Mistree, F., 1996, "A Procedure for Robust Design: Minimizing Variations Caused by Noise Factors and Control Factors," ASME J. Mech. Des., **118**, pp. 478–485.
[29] Scott, M. J., and Antonsson, E. K., 2005, "Compensation and Weights for Trade-Offs in Engineering Design: Beyond the Weighted Sum," ASME J. Mech. Des., **127**, pp. 1045–1055.
[30] Das, I., and Dennis, J. E., 1997, "A Closer Look at Drawbacks of Minimizing Weighted Sum of Objectives for Pareto Set Generation in Multicriteria Optimization Problems," Struct. Optim., **14**, pp. 63–69.
[31] Chen, W., Wiecek, M. M., and Zhang, J., 1998, "Quality Utility: A Compromise Programming Approach to Robust Design," *ASME DETC98/DAC5601.*
[32] Fonseca, C. M., and Fleming, P. J., 1993, "Genetic Algorithm for Multi-Objective Optimization: Formulation, Discussion and Generalization," *Proceedings of the Fifth International Conference on Genetic Algorithms*, S. Forrest, ed., San Mateo, CA.

[33] Horn, J., Nafploitis, N., and Goldberg, D. E., 1994, "A Niched Pareto Genetic Algorithm for Multi-Objective Optimization," *Proceedings of the First IEEE Conference on Evolutionary Computation*, Z. Michalewicz, ed., Piscataway, NJ.
[34] Zitler, E., and Thiele, L., 1999, "Multiobjective Evolutionary Algorithms: A Comparitive Case Study and the Strength Pareto Approach," IEEE Trans. Evol. Comput., **3**, pp. 257–271.
[35] Fieldsend, J. E., Everson, R. M., and Singh, S., 2003, "Using Unconstrained Elite Archives for Multiobjective Optimization," IEEE Trans. Evol. Comput., **7**, pp. 305–323.
[36] Deb, K., Pratap, A., Agarwal, S., and Meyarivan, T., 2002, "A Fast and Elitist Multiobjective Genetic Algorithm: NSGA-II," IEEE Trans. Evol. Comput., **6**, pp. 182–197.
[37] Hicks, R. M., and Henne, P. A., 1998, "Wing Design by Numerical Optimisation," J. Aircr., **15**(7), pp. 407–412.
[38] Wu, H. Y., Yang, S., and Liu, F., 2003, "Comparison of Three Geometric Representation of Airfoils for Aerodynamic Optimization," AIAA Pap., 2003–4095.
[39] Shahpar, S., and Lapworth, L., 2003, "Parametric Design and Rapid Meshing Systems for Turbomachinery Optimisation," *ASME-GT2003-38698*.
[40] Moinier, P., 1999, "Algorithm Developments for an Unstructured Viscous Flow Solver," Ph.D. thesis, Oxford University, Oxford.
[41] Moinier, P., Muller, J. D., and Giles, M. B., 1999, "Edge-Based Multigrid and Preconditioning for Hybrid Grids," AIAA Pap., 99–3339.
[42] Keane, A. J., and Nair, P. B., 2005, *Computational Approaches for Aerospace Design*, Wiley, New York.
[43] Matheron, G., 1963, "Principles of Geostatistics," Econ. Geol., **58**, pp. 1246–1266.
[44] Neal, R. M., 1996, *Bayesian Learning for Neural Networks*, Springer, New York.
[45] MacKay, D. J. C., 1997, "Gaussian Processes-A Replacement for Supervised Neural Networks," Tutorial lecture Notes for NIPS, at http://www.inference.phy.cam.ac.uk/mackay/abstracts/gp.html, 1997.
[46] Jones, D. R., Schonlau, M., and Welch, W. J., 1998, "Efficient Global Optimization of Expensive Black-Box Functions," J. Global Optim., **13**(4), pp. 455–492.
[47] Nair, P. B., Choudhary, A., and Keane, A. J., 2001, "A Bayesian Framework for Uncertainty Analysis Using Deterministic Black-Box Simulation Code," AIAA Pap., 2001–1676.
[48] Keane, A. J., 2003, "Wing Optimization Using Design of Experiment, Response Surface, and Data Fusion Methods," J. Aircr., **40**, pp. 741–750.
[49] Sacks, J., Welch, W. J., Mitchell, T. J., and Wynn, H. P., 1989, "Design and Analysis of Computer Experiments," Stat. Sci., **4**(4), pp. 409–435.
[50] Schonlau, M., 1997, "Computer Experiments and Global Optimization," Ph.D. thesis, University of Waterloo.
[51] Chen, W., Jin, R., and Sudjianto, A., 2005, "Analytical Variance-Based Global Sensitivity Analysis in Simulation-Based Design Under Uncertainty," ASME J. Mech. Des., **127**, pp. 875–884.
[52] Sobol, I. M., 1994, *A Primer for the Monte Carlo Method*, CRC Press, Boca Raton.
[53] Athan, T. W., and Papalambros, P. Y., 1996, "A Note on Weighted Criteria Methods for Compromise Solutions in Multi-Objective Optimization," Eng. Optimiz., **27**(2), pp. 155–176.
[54] Koski, J., 1985, "Defectiveness of Weighting Method in Multicriterion Optimization of Structures," Commun. Appl. Numer. Methods, **1**, pp. 333–337.
[55] Deb, K., 1999, "Multi-Objective Genetic Algorithms: Problem Difficulties and Construction of Test Functions," Evol. Comput., **7**, pp. 205–230.